

# Performance of LaNi<sub>4.7</sub>Sn<sub>0.3</sub> Metal Hydride Electrodes in Sealed Cells

A. Hightower<sup>a</sup>, C. K. Witham<sup>a</sup>, R. C. Bowman Jr.<sup>b</sup>, B. V. Ratnakumar<sup>b</sup>,  
B. Fultz<sup>a</sup>, B. Czajkowski<sup>c</sup>, L. Zhang<sup>c</sup>, D. Singh<sup>c</sup>,  
M. Klein<sup>c</sup>, and L. Huston<sup>c</sup>

<sup>a</sup>California Institute of Technology, Mail Stop 138-78, Pasadena, CA 91125

<sup>b</sup>Jet Propulsion Laboratory, 4800 Oak Grove Drive, Pasadena, CA 91109

<sup>c</sup>Energizer Power Systems, Highway 441 N, Gainesville, FL 32614-7114

## ABSTRACT

Cycle life and kinetics studies were performed on sealed nickel metal hydride electrochemical cells with anodes of LaNi<sub>4.7</sub>Sn<sub>0.3</sub> and of a standard misch metal alloy. The modest increase in cell capacity of the LaNi<sub>4.7</sub>Sn<sub>0.3</sub> alloy at higher rates of discharge suggests improved kinetics. AC Impedance studies as a function of cycle life indicate the onset of cell failure. Self-discharge rates in sealed cells correlate with alloy plateau pressures measured by gas phase isotherms and internal cell pressures. Cycle life of the LaNi<sub>4.7</sub>Sn<sub>0.3</sub> was inferior to cells of standard misch metal formulation Mm(NiAlCoMn)<sub>5</sub>.

## INTRODUCTION

Since the mid-1980's, studies on metal hydrides as anodes in nickel metal hydride (NiMH) batteries have moved from fundamental scientific investigations to product-based industrial efforts. Metal hydrides (MH) now have widespread application as negative electrodes in rechargeable batteries for the consumer electronics industry. The present investigation focused on electrochemical properties of metal hydride alloys based on LaNi<sub>5</sub>, denoted generically as "AB<sub>5</sub>" alloys.

Commercial AB<sub>5</sub> metal hydride alloys in rechargeable batteries include substantial substitutions of other elements for La and for Ni. To reduce cost and improve cycle life, La is replaced with misch metal (Mm) which is a reduced ore of a variety of rare earth elements. Sakai, et al. (1) studied various ternary substitutions for Ni in LaNi<sub>5</sub>, and reported that the cycle life improves with the ternary substituents in the order Mn < Ni < Cu < Cr < Al < Co. The beneficial effects of Co have led to large Co substitutions for Ni in commercial AB<sub>5</sub> alloys. Higher costs and limited availability of the strategic element Co make it worthwhile to

investigate alternate elements for substitution with Ni. Sn has proven itself as a viable candidate for promoting cycle life while retaining cell capacity in laboratory tests.

The characteristics of LaNi<sub>4.7</sub>Sn<sub>0.3</sub> have been well documented in laboratory cells. Previous studies by the Caltech /JPL group on LaNi<sub>5</sub> substituted with 0 - 8.3 at.% Sn for Ni revealed trends between alloy performance and Sn composition (2,3). Kinetics, thermodynamics, and cycle life of LaNi<sub>5.0-x</sub>Sn<sub>x</sub> (x = 0 - 0.5) were determined by electrochemical and gas-phase studies. The microstructures of these alloys were determined by X-ray diffractometry and TEM (4-6). Compared to other ternary alloys, LaNi<sub>5.0-x</sub>M<sub>x</sub> (M = Al, Ga, In, Si), Sn-containing alloys showed the longest cycle life. The optimal concentration of Sn, with respect to a balance among cycle life, capacity and kinetics, was found to be in the range of LaNi<sub>5.0-x</sub>Sn<sub>x</sub>, x = 0.25 - 0.3. The reason for the improved cycle life may be related to the strong chemical bonding between La and Sn (7).

These previous results have prompted us to investigate the performance of Sn-substituted alloys in sealed cells. Here we report results of studies on the kinetics, capacity, and cycle life of sealed cells of

LaNi<sub>4.7</sub>Sn<sub>0.3</sub>. The performance of these alloys, as-cast and after annealing, is compared to a standard commercial AB<sub>5</sub> alloy.

## EXPERIMENTAL

The AB<sub>5</sub> alloys used in this study were produced by vacuum induction melting of elemental raw materials of commercial purity (99+%). The Sn-containing alloy was melted as a 6 kg heat. Half of the ingot was annealed for 72 hours at 950°C in an argon atmosphere. The partial ingots were then mechanically crushed to < 75 microns powder. The oxygen content of the powder obtained from the heat-treated ingot was 0.07 wt.%. The chemical composition as determined by Induction Coupled Plasma (ICP) Atomic Emission Spectroscopy was LaNi<sub>4.58</sub>Sn<sub>0.3</sub>, or just slightly sub-stoichiometric. The commercial AB<sub>5</sub> alloy used as the control has the nominal composition MmNi<sub>3.6</sub>Co<sub>0.7</sub>Al<sub>0.4</sub>Mn<sub>0.3</sub>, where Mm is La-rich misch metal, a mixture of light rare earth elements, with the approximate atomic ratio of La<sub>0.53</sub>Ce<sub>0.32</sub>Pr<sub>0.04</sub>Nd<sub>0.11</sub>. The heat size was in excess of 300 kg and the ingots were mechanically crushed to < 75 microns powder. Chemical control is ±0.2 wt. % for each of the B-side elements (Co, Al and Mn).

AA NiMH cells were assembled at Energizer by winding thin planar Ni(OH)<sub>2</sub> sinter-type electrodes and pasted MH electrodes between a layer of battery-grade nylon separator. The MH electrodes used in this study were fabricated using pulverized, < 75 microns, MH alloy powder, admixed with a small (<2%) amount of binder and solvent, applied to thin nickel-plated perforated steel substrate, dried, calendared and sized. Approximately 7 g of MH alloy was used per electrode. The same alloy weight was used for all MH compositions. Electrolyte consisting of KOH with small additions of NaOH and LiOH was added prior to cell sealing. The cell capacity was set by the positive electrode at approximately 1000 mAh for all of the cells assembled.

Cycling of the AA NiMH cells at Energizer was performed on automated battery cycling equipment. Cycling conditions were 1C rate (1000 mA) charge to a negative change in voltage ("negative delta V") or until 38°C was reached (which ever comes first), followed by a C/10 charge rate (approximately 2 hours) to ensure complete cell charging and to fill a 3 hour test time window. Cells rested 2 minutes after charge and then discharged at 1C rate to 0.9 V. Following discharge, cells were given a 1 hour rest before recharge.

The cycling of cells at JPL was carried out with an automatic battery cycler made by Arbin Corp., College Station, TX. The cycling conditions included a discharge step at 1C rate to 0.9 V. After a two minute rest period, charging was done in two steps. Initial charging at 1C rate was performed for a maximum of one hour or to 1.6 V followed by charge step at C/10 rate for half an hour. This procedure gave a charge/discharge ratio of 1.25 or a cutoff voltage of 1.6 V, whichever came first.

Gas pressure and analysis were performed on laboratory equipment that punctures a cell, releases cell gases into a pre-measured volume, measures pressure using a Dynisco pressure transducer, calculates internal cell pressure and sends a sample of the captured gas to a Gow-Mac Gas Chromatograph (Series 500) for analysis. Gas pressure and composition were measured immediately after removing the cells from charge.

Self discharge rates were carried out at JPL using the same charge and discharge conditions described above for cell cycling. Annealed LaNi<sub>4.7</sub>Sn<sub>0.3</sub> and Mm(NiAlCoMn)<sub>5</sub> cells were subjected to five cycles to establish a baseline capacity. The cells were then allowed to sit at 25°C and 45°C for several days. Their discharge capacities were then measured and normalized to initial capacity.

AC impedance measurements were carried out with the EG&G 273 Potentiostat and Solartron 1255 Frequency Response Analyzer, using EG&G Impedance software 388.

## RESULTS & DISCUSSION

### *Isotherms*

Figure 1 displays isotherm data of gas-phase desorption at 45°C of a typical Mm(NiAlCoMn)<sub>5</sub> and LaNi<sub>4.7</sub>Sn<sub>0.3</sub> in the as-cast and annealed conditions. The isotherm of the annealed Sn alloy displays a flatter plateau and larger capacity relative to the Mm(NiAlCoMn)<sub>5</sub>. The upward slope of the isotherm for the as-cast Sn alloy can be attributed to the chemical inhomogeneity of the material. An inhomogeneous distribution of Sn in the as-cast alloy will lead to some regions favorable for hydrogen occupancy but other regions less so.

### *Self Discharge*

A correlation between hydride desorption pressure and self discharge ratios have been reported by Anani, et al (8). A lower self discharge for annealed LaNi<sub>4.7</sub>Sn<sub>0.3</sub> alloys was suggested by the gas phase isotherms. The lower H<sub>2</sub> pressure at greater hydrogen to MH ratios (H/f.u. > 3) indicates the

greater stability of hydrogen in the  $\text{LaNi}_{4.7}\text{Sn}_{0.3}$  alloys. The flat isotherms translate into smaller gradients in the hydrogen chemical potential and thus reduced hydrogen evolution. Results of self discharge tests are shown in figure 2.

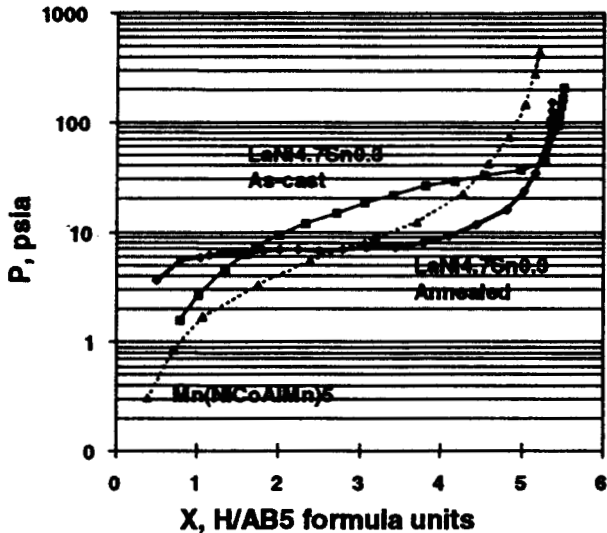


Fig. 1: Gas phase desorption isotherms of the as-cast  $\text{LaNi}_{4.7}\text{Sn}_{0.3}$  alloy, annealed  $\text{LaNi}_{4.7}\text{Sn}_{0.3}$ , and the commercial alloy of typical  $\text{Mm}(\text{NiAlCoMn})_5$  composition measured at  $45^\circ\text{C}$ .

As expected, we consistently find lower self discharge in annealed  $\text{LaNi}_{4.7}\text{Sn}_{0.3}$  sealed cells (AA - size) as compared to  $\text{Mm}(\text{NiAlCoMn})_5$  cells. The degree of self discharge increases with

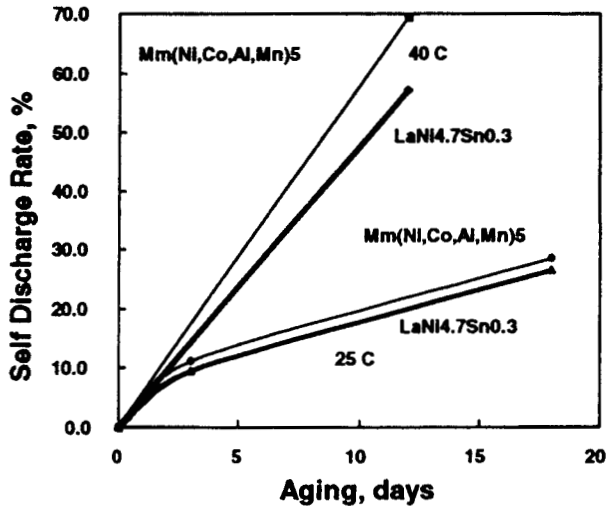


Fig. 2: Self discharge data showing loss in stored electrochemical capacity versus time for annealed  $\text{LaNi}_{4.7}\text{Sn}_{0.3}$  alloy and commercial alloy of typical  $\text{Mm}(\text{NiAlCoMn})_5$  composition measured at  $25^\circ\text{C}$  and  $45^\circ\text{C}$ .

temperature, with the  $\text{LaNi}_{4.7}\text{Sn}_{0.3}$  being less sensitive to this effect. Self discharge can also be influenced by the by-products of nylon separator degradation and nitrates remaining in the positive Ni electrode. However, these cells were fabricated with identical procedures and thus the differences in self-discharge shown in figure 2 reflect the nature of the MH electrode material.

#### Rate Measurements

It is difficult to infer negative electrode kinetics from the performance measurements of commercial sealed cells. This is because the cells are purposely built with an excess of negative electrode (i.e., positive limited to reduce  $\text{H}_2$  gassing problems). Cell capacity variations are shown in figure 3 as a function of discharge current up to  $3\text{C}$ . Groups of 2 to 5 cells were tested to obtain these results. The higher capacity evidenced for the  $\text{LaNi}_{4.7}\text{Sn}_{0.3}$  at all discharge rates, may be indicative of improved kinetics for this alloy. Nevertheless, the difference in rate capacity of the  $\text{LaNi}_{4.7}\text{Sn}_{0.3}$  and  $\text{Mm}(\text{NiAlCoMn})_5$  electrodes is not substantial.

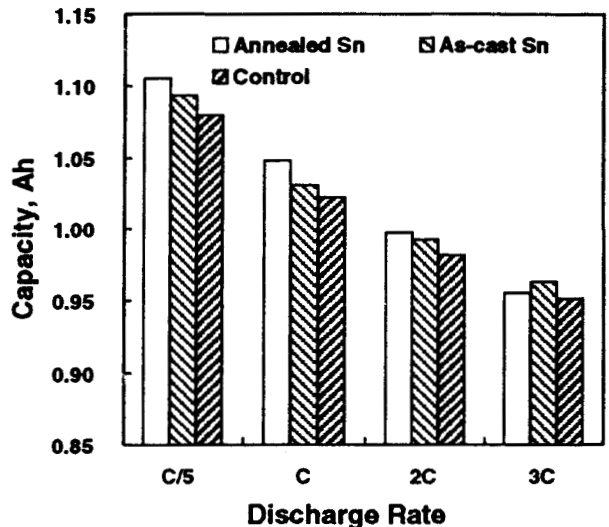


Fig. 3: Electrochemical capacities of AA cells measured at different rates of discharge.

#### Pressure

Pressures of gases evolved from the charging of the sealed cells at  $1\text{C}$  rate were measured. There were similar amounts of total gases evolved from all cells. Figure 4 shows that the amount of  $\text{H}_2$  gas evolved from each cell increases with the time of charge. The reduced hydrogen emission of the annealed Sn alloy follows from the reduction in plateau pressure. The as-cast  $\text{LaNi}_{4.7}\text{Sn}_{0.3}$ , with its more inhomogeneous Sn distribution, showed greater hydrogen evolution.

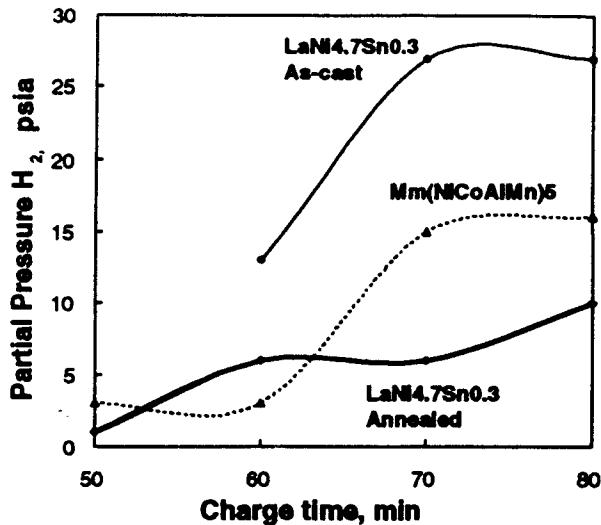


Fig. 4: Partial pressure of H<sub>2</sub> gas evolved from cells during different charging times at 1C rate.

#### Cycle Life

Cycle life tests on sealed cells of as-cast and annealed LaNi<sub>4.7</sub>Sn<sub>0.3</sub> are compared to Mm(NiAlCoMn)<sub>5</sub> control cells in Figs. 5 and 6. These experiments were conducted at JPL and Energizer under different cycling conditions and provided the data for figures 5 and 6, respectively.

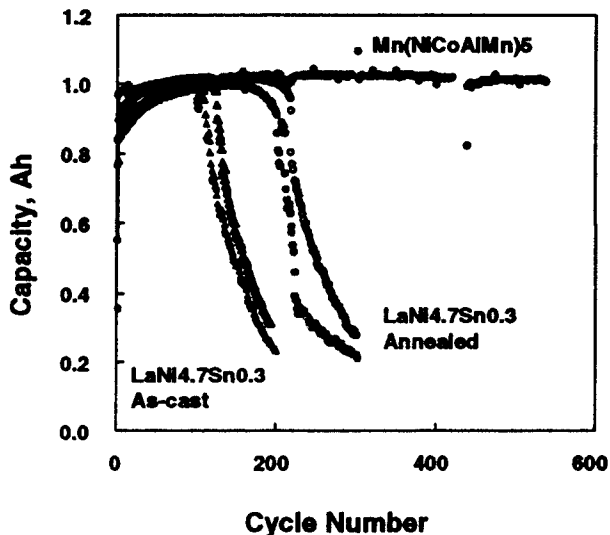


Fig. 5: Cycle life for sealed cells containing as-cast LaNi<sub>4.7</sub>Sn<sub>0.3</sub> alloy, annealed LaNi<sub>4.7</sub>Sn<sub>0.3</sub>, and the commercial alloy of typical Mm(NiAlCoMn)<sub>5</sub> composition measured at room temperature. Two cells of each were measured at JPL.

The as-cast and annealed LaNi<sub>4.7</sub>Sn<sub>0.3</sub> cells exhibit shorter activation times and more rapid degradation compared to control cells in both measurements.

The Mm(NiAlCoMn)<sub>5</sub> alloys display superior cycle life to the LaNi<sub>4.7</sub>Sn<sub>0.3</sub> alloys. It is widely accepted (9) that the substitution of Co and Al for Ni inhibit volume dilatation during hydrogen absorption, and thereby improves cycle life. It has also been proposed that the Ce (10) and Nd (9) present in the misch metal promotes beneficial passivating films. These passivating films protect the rare earth elements from the corrosive electrolyte. We suggest that the lifetimes of LaNi<sub>4.7</sub>Sn<sub>0.3</sub> could be improved with the substitution of misch metal for La. Encouraging results from Ce additions have been reported previously (11).

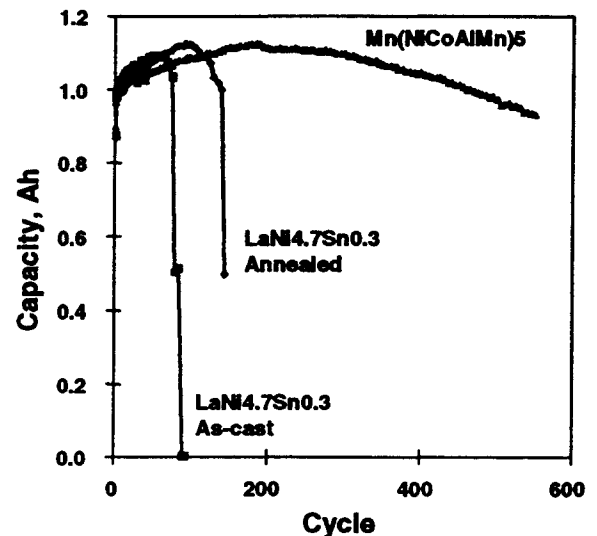


Fig. 6: Cycle life data for sealed cells containing as-cast LaNi<sub>4.7</sub>Sn<sub>0.3</sub> alloy, annealed LaNi<sub>4.7</sub>Sn<sub>0.3</sub>, and the commercial alloy of typical Mm(NiAlCoMn)<sub>5</sub> composition. Measurements were carried out at Energizer.

#### AC Impedance

The LaNi<sub>4.7</sub>Sn<sub>0.3</sub> and Mm(NiAlCoMn)<sub>5</sub> sealed cells differ considerably in their series Ohmic resistance during cycling, as shown in figure 7. The Ohmic resistance of sealed cells, generated from the interfaces between electrode, electrolyte, and leads, was measured by AC impedance spectrometry. The initial decrease seen in this parameter could be due to the decrepitation of the metal hydride alloy particles, which results in an enhanced surface area (and thus reduced resistance). The subsequent increase in the resistance may be an indication of the corrosion and passivation processes, which

might be responsible for the shorter cycle life of the cells with Sn-based alloy.

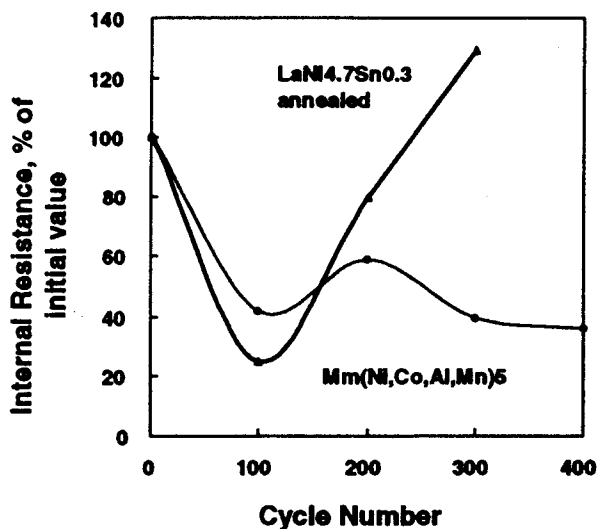


Fig. 7: Cell internal resistances vs. cycle number determined by AC impedance studies on annealed  $\text{LaNi}_{4.7}\text{Sn}_{0.3}$  and the commercial  $\text{Mm}(\text{Ni,Co,Al,Mn})_5$ .

## CONCLUSIONS

Our studies have found  $\text{LaNi}_{4.7}\text{Sn}_{0.3}$  alloys to possess limited utility in rechargeable nickel metal hydride batteries. The enhancements relative to  $\text{Mm}(\text{NiAlCoMn})_5$  in kinetics and reduction in self discharge observed in laboratory cells have been demonstrated in sealed cells. The  $\text{LaNi}_{4.7}\text{Sn}_{0.3}$  cells exhibited lower self discharge and greater capacities at higher rates of discharge compared to cells of the standard misch metal composition  $\text{Mm}(\text{NiAlCoMn})_5$ . The  $\text{LaNi}_{4.7}\text{Sn}_{0.3}$  cells did not display cyclic lifetimes comparable to the  $\text{Mm}(\text{NiAlCoMn})_5$  cells. Hence, the enhancements in lifetime from Sn substitution alone, which were clearly demonstrated in previous half-cell electrode studies (3,7) and attributed to the strong chemical bonding between La and Sn, was not found to be as effective as the combined contributions in commercial  $\text{Mm}(\text{NiAlCoMn})_5$  alloys. The next logical step is to investigate improvements to the lifetimes of the  $\text{LaNi}_{4.7}\text{Sn}_{0.3}$ , by substituting Ce for a portion of the La. We expect that the surface effects from passivating films and changes to the alloy volume expansion on hydriding (11) will improve cycle life for reasons independent of the beneficial effects of Sn. However, substitution of Ce may reduce capacity through formation of other

impurity phases. This behavior will be the subject of future studies.

## ACKNOWLEDGMENTS

This work was partially carried out at the Jet Propulsion Laboratory, under contract with the National Aeronautics and Space Administration. And was supported by DOE Basic Energy Sciences grant DE-FG03-94ER14493.

## REFERENCES

1. T. Sakai, K. Oguru, H. Miyamura, N. Kuriyama, A. Kato and H. Ishikawa, *J. Less Common Metals*, **161**, 193 (1990).
2. R.C. Bowman, Jr., C.H. Luo, C.C. Ahn, C.K. Witham and B. Fultz, *J. Alloys and Compounds*, **217**, 185 (1995).
3. B.V. Ratnakumar, C. Witham, R. C. Bowman, Jr., A. Hightower, and B. Fultz, *J. of Electrochem. Soc.*, **143**, 2578 (1996).
4. M. Mendelsohn, D. Gruen, A. Dwight, *Inorg. Chem.* **18**, 3343 (1979).
5. J. S. Cantrell, T.A. Beiter and R.C. Bowman, Jr., *J. Alloys and Compounds*, **207/208**, 372 (1994).
6. M. Wasz, R.B. Schwarz, S. Srinivasan and M.P.S. Kumar, in *Materials for Electrochemical Energy Storage and Conversion - Batteries, Capacitors, and Fuel Cells*, Symposium Proceedings of The Materials Research Society, San Francisco, CA Vol. 93, pp. 237-242, Spring (1995).
7. C. Witham, R. C. Bowman, Jr., B.V. Ratnakumar, and B. Fultz, in *AB<sub>5</sub> Metal Hydride Alloys for Alkaline Rechargeable Cells.*, Proc. 11<sup>th</sup> Annual Battery Conference on Applications and Advances, Long Beach, CA (Inst. Electrical Electronic Eng., Piscataway, NJ), (1996), pp. 129-134.
8. A. Anani A. Visintin, S. Srinivasan, A. J. Appleby, J. J. Reilly, and J. R. Johnson *Electrochem. Soc. Proc.* **92-5**, p. 105 (1992).
9. J. J. G. Willems, *Philips J. Res.*, **39** (Suppl. 1), 1 (1984); J.J.G. Willems and K.H. J. Buschow, *J. Less Common Metals*, **129**, 13 (1987).
10. T. Sakai, T. Hazama, H. Miyamura, N. Kuriyama, A. Kato and H. Ishikawa, *J. Less Common Metals*, **172-174**, 1175 (1991).
11. G. D. Adzic, J. R. Johnson, J. J. Reilly, J. McBreen, S. Mukerjee, M. P. Sridhar Kumar, W. Zhang, S. Srinivasan, *J. Electrochem. Soc.* **142**, 3429 (1995).